miR-19 is a key oncogenic component of *mir-17-92*

Virginie Olive,[1,5] Margaux J. Bennett,[1,5] James C. Walker,[1] Cong Ma,[1] Iris Jiang,[1] Carlos Cordon-Cardo,[2] Qi-Jing Li,[3] Scott W. Lowe,[4] Gregory J. Hannon,[4,7] and Lin He[1,6]

[1]Division of Cellular and Developmental Biology, Department of Molecular and Cell Biology, University of California at Berkeley, Berkeley, California 94705, USA; [2]Irving Cancer Research Center, New York, New York 10032, USA; [3]Department of Immunology, Duke University Medical Center, Durham, North Carolina 27710; [4]Watson School of Biological Sciences, Cold Spring Harbor Laboratory, Cold Spring Harbor, New York 11724, USA

Recent studies have revealed the importance of multiple microRNAs (miRNAs) in promoting tumorigenesis, among which *mir-17-92/Oncomir-1* exhibits potent oncogenic activity. Genomic amplification and elevated expression of *mir-17-92* occur in several human B-cell lymphomas, and enforced *mir-17-92* expression in mice cooperates with *c-myc* to promote the formation of B-cell lymphomas. Unlike classic protein-coding oncogenes, *mir-17-92* has an unconventional gene structure, where one primary transcript yields six individual miRNAs. Here, we functionally dissected the individual components of *mir-17-92* by assaying their tumorigenic potential in vivo. Using the *Eµ-myc* model of mouse B-cell lymphoma, we identified *miR-19* as the key oncogenic component of *mir-17-92*, both necessary and sufficient for promoting *c-myc*-induced lymphomagenesis by repressing apoptosis. The oncogenic activity of *miR-19* is at least in part due to its repression of the tumor suppressor *Pten*. Consistently, *miR-19* activates the Akt–mTOR (mammalian target of rapamycin) pathway, thereby functionally antagonizing *Pten* to promote cell survival. Our findings reveal the essential role of *miR-19* in mediating the oncogenic activity of *mir-17-92*, and implicate the functional diversity of *mir-17-92* components as the molecular basis for its pleiotropic effects during tumorigenesis.

MicroRNAs (miRNAs) encode small, regulatory RNAs that control gene expression predominantly through post-transcriptional repression (Ambros 2004; Zamore and Haley 2005; Bartel 2009). Nascent transcripts from miRNA genes (pri-miRNAs) contain one or multiple unique stem–loop structures. Mature miRNAs, ranging from 18 to 24 nucleotides (nt) in length, are initially embedded within one arm of the hairpin stems. These pri-miRNAs are processed sequentially by the ribonuclease III enzymes Drosha and Dicer to yield the mature miRNA duplexes (Kim et al. 2009). As the mature duplex is formed, the miRNA strand is then incorporated into the RNA-induced silencing complex (RISC) to mediate post-transcriptional regulation of specific mRNAs, primarily through mRNA degradation and/or translational repression (Filipowicz et al. 2008). The target recognition by miRNAs is achieved through imperfect complementarity. The seed region of the mature miRNA (nucleotides 2–8) is often complementary to sites within the target mRNAs, forming a "seed match" in an otherwise imperfect base-pairing (Bartel 2009). The small size of miRNAs, combined with imperfect target recognition, provide miRNAs with the enormous capacity and versatility to act as global gene regulators in diverse developmental and physiological processes. Recent bioinformatic predictions and several experimental validations also suggest that each miRNA is likely to regulate hundreds of mRNA targets and fine-tune their expression in a cell type-dependent and context-dependent manner (Baek et al. 2008; Selbach et al. 2008; Chi et al. 2009).

The connection between miRNAs and cancer was first implicated by their frequent genomic alteration and dysregulated expression in various human tumors (Calin et al. 2004; Lu et al. 2005; He et al. 2007b). Multiple miRNAs were subsequently identified to promote or suppress oncogenesis, presumably by modulating gene expression in the oncogenic and tumor suppressor networks (He et al. 2005, 2007a; Johnson et al. 2005; Kumar et al. 2008; Kota et al. 2009). One of the first oncogenic miRNAs identified was *mir-17-92* (also known as *oncomir-1*), a miRNA polycistron with pleiotropic functions in cell

Olive et al.

survival, proliferation, differentiation, and angiogenesis (Hayashita et al. 2005; He et al. 2005; Lu et al. 2005; O'Donnell et al. 2005; Dews et al. 2006; Ventura et al. 2008). *mir-17-92* is the primary target of the genomic amplification 13q31 that occurs in Burkitt's lymphoma, diffuse large B-cell lymphoma (DLBCL), mantle cell lymphoma, follicular lymphoma, and several other solid tumor types (Ota et al. 2004; He et al. 2005; Tagawa and Seto 2005; Tagawa et al. 2007; Inomata et al. 2009; Navarro et al. 2009). Additionally, *mir-17-92* is highly expressed in a range of hematopoietic malignancies, particularly in B-cell lymphomas (Lu et al. 2005; Tagawa and Seto 2005; Navarro et al. 2009). Although transgenic mice with moderate *mir-17-92* overexpression only develop lymphoproliferative phenotypes (Xiao et al. 2008), enforced high-level expression of *mir-17-92*, in conjunction with *c-myc*, has potent transformation potential in mouse B cells in vivo, largely due to its ability to repress apoptosis (He et al. 2005) This observation is consistent with the recurring *mir-17-92* amplifications in *MYC*-rearranged Burkitt's lymphomas and DLBCLs in humans (Tagawa et al. 2007). The survival effect of *mir-17-92* is also evident in the normal development of the B-cell compartment, as *mir-17-92* deficiency leads to premature cell death during pro-B-to-pre-B transition (Ventura et al. 2008).

Unlike classic protein-coding oncogenes, where one transcript generally gives rise to one protein product, the *mir-17-92* miRNA cluster produces a single polycistronic primary transcript that yields six individual mature miRNAs. The distinct mature miRNA sequence of these

mir-17-92 components dictates the specificity of their target regulation, and ultimately can determine the functional specificity. Here we report the functional dissection of *mir-17-92* in the context of B-cell transformation in vivo, and reveal the essential role of *miR-19* in mediating the oncogenic activity of *mir-17-92*. In the *Eμ-myc* model of Burkitt's lymphoma, *miR-19* is both necessary and sufficient for *mir-17-92* to promote *c-myc*-induced B lymphomagenesis. The oncogenic activity of *miR-19* is at least in part mediated by the PI3K (phosphatidylinositol 3-kinase)–Akt–mTOR (mammalian target of rapamycin) pathway, as enforced *miR-19* expression dampens the expression of the tumor suppressor *Pten*, thus activating the Akt–mTOR signaling to promote cell survival. Our findings demonstrate the functional diversity of *mir-17-92* components, and characterize the key molecular mechanism through which the *mir-17-92* polycistron promotes malignant transformation in the B-cell compartment.

Results

mir-17-92 encodes a miRNA polycistron that yields six individual components

The *mir-17-92* miRNA cluster produces a single polycistronic primary transcript that yields six mature miRNAs: *miR-17*, *miR-18a*, *miR-19a*, *miR-20a*, *miR-19b*, and *miR-92a* (Fig. 1A). This unique structural feature of *mir-17-92*, shared by a large number of miRNA genes in mammalian genomes, may constitute the molecular basis for its pleiotropic functions in a cell type-dependent
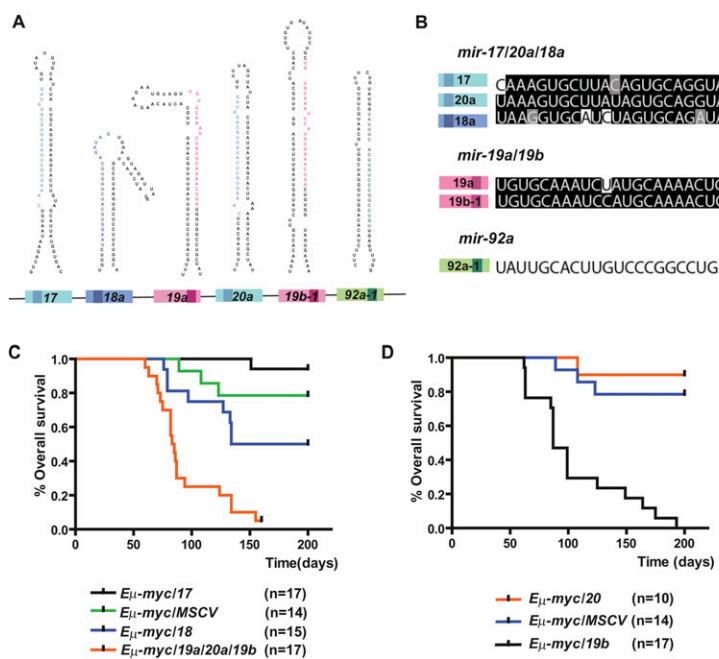
Figure 1. *miR-19b* phenocopies the oncogenic effects of *mir-17-92* in the *Eμ-myc* model. (*A*) Gene structure of the *mir-17-92* polycistronic cluster. (Light-colored boxes) Pre-miRNAs; (dark-colored boxes) mature miRNAs. Homologous miRNA components are indicated by the same or similar colors. (*B*) *mir-17-92* components belong to three miRNA families: *miR-17/20a/18* (blue), *miR-19* (red), and *miR-92a* (green). Mature miRNA sequence alignments are shown for each family. Based on sequence identity, *miR-17* and *miR-20a* are closely related homologs, sharing significant sequence identity with *miR-18a*, but containing a slightly different seed (74% identity among all three). *miR-19a* and *miR-19b* differ by a single nucleotide at position 11, and are likely to regulate the same mRNA targets (96% identity). *miR-92a* has a unique seed sequence that distinguishes it from other components. (*C*) The *mir-19a/20a/19b* subcluster accelerates *c-myc*-induced lymphomagenesis. Irradiated mice reconstituted with the *Eμ-myc/+* HSPCs overexpressing *miR-17*, *miR-18a*, *mir-19a/20a/19b*, or a MSCV control vector were monitored weekly beginning 4 wk post-transplantation. The Kaplan-Meier curves represent percentage of overall survival. (*D*) *miR-19b* accelerates *c-myc*-induced lymphomagenesis. The *mir-19a/20/19b* subcluster was further divided into *miR-19b* and *miR-20a*, each overexpressed in the *Eμ-myc/+* HSPCs before transplantation into lethally irradiated recipient animals. Reconstituted mice were monitored weekly starting 4 wk post-transplantation. The Kaplan-Meier curve indicates *miR-19b* has a strong oncogenic effect.

and context-dependent manner. Based on sequence homology, the six *mir-17-92* components can be categorized into three miRNA families: *miR-17/20a/18a*, *miR-19a/19b*, and *miR-92a* (Fig. 1B). *miR-17* and *miR-20a* miRNAs are closely related homologs, differing by 2 nt outside the seed sequence (Fig. 1B). A related miRNA *miR-18a* has a similar yet not identical seed region, but shares significant sequence identity with *mir-17/20a* overall (Fig. 1B). The second miRNA family contains *miR-19a* and *miR-19b*, which differ only by a single nucleotide at position 11, a region minimally important for target recognition (Fig. 1B; Lewis et al. 2003, 2005; Farh et al. 2005; Grimson et al. 2007). Finally, the unique seed region of *miR-92a* distinguishes it from all of the other *mir-17-92* components (Fig. 1B). All six *mir-17-92* miRNAs can repress many target mRNAs either cooperatively or individually; both mechanisms could lead to cell type-dependent and context-dependent functional readout.

miR-19 *exhibits potent oncogenic activity in the* Eμ-myc *model*

Previously, we chose the *Eμ-myc* model of Burkitt's lymphoma to evaluate the oncogenic activity of *mir-17-92* in vivo because genomic amplification and up-regulated expression of *mir-17-92* were both observed in human Burkitt's lymphomas (Tagawa et al. 2007). Recent studies also indicated the association between recurring *mir-17-92* genomic amplification and *MYC* rearrangement in Burkitt's lymphomas and DLBCLs, further implicating a functional cooperation between these two lesions (Tagawa et al. 2007). The *Eμ-myc* transgenic mice carry a *c-myc* oncogene driven by the immunoglobulin heavy-chain enhancer (*Eμ*), which is a powerful system in Burkitt's lymphoma. These mice exhibit *c-myc* overexpression specifically in the B-cell lineage, and ultimately acquire late-onset B-cell lymphomas with a latency of ~6 mo (Adams et al. 1985). To examine the oncogenic potentials of any candidate miRNA, the *Eμ-myc*/+ hematopoietic stem and progenitor cells (HSPCs) can be infected with murine stem cell viruses (MSCVs) overexpressing the miRNA, and then transplanted into lethally irradiated recipient animals (Supplemental Fig. S1B; Schmitt et al. 2000). The oncogenic potential can be evaluated by the acceleration of *c-myc*-induced lymphomagenesis in this adoptive transfer model (Supplemental Fig. S1B).

The first evidence that individual *mir-17-92* components may contribute differently to its oncogenic potential comes from our previous observation, in which *mir-17-19b*, a truncated *mir-17-92* cluster lacking *miR-92a* (Supplemental Fig. S1A), can greatly accelerate *c-myc*-induced tumorigenesis in the *Eμ-myc* model (He et al. 2005). The fact that *miR-92a* is dispensable for the oncogenic activity prompted us to further divide the *mir-17-19b* cluster to functionally dissect the oncogenic potentials of each individual miRNA component (Supplemental Fig. S1A).

We initially divided the oncogenic *mir-17-19b* miRNA polycistron into three subclusters: *miR-17*, *miR-18a*, and *mir-19a/20a/19b* (Supplemental Fig. S1A). Overexpres-

sion of the control vector (MSCV) or *miR-17* in this adoptive transfer model had minimal oncogenic effects, causing late-onset B lymphomas with incomplete penetrance (Fig. 1C). In contrast, animals coexpressing *mir-19a/20a/19b* and *c-myc* developed highly malignant, early-onset B lymphomas, with a median survival at 84 d post-transplantation (*P* < 0.0001, log rank test) (Fig. 1C). Interestingly, *miR-18a* overexpression caused a moderate acceleration of lymphomagenesis in the *Eμ-myc* model (Fig. 1C). Although it is unlikely that *miR-18a* is the major oncogenic component of *mir-17-19b*, it may play accessory roles to facilitate *miR-19a/20a/19b* to promote malignant transformation in the *Eμ-myc* model. Retroviruses driving *mir-17-19b* and each of the subclusters had similar levels of overexpression, indicating that the observed difference in oncogenic effects reflected true functional differences among *mir-17-92* components, rather than differences in expression level (data not shown).

The three miRNAs encoded by *mir-19a/20a/19b* belong to two distinct families: *miR-19* (including *miR-19a* and *miR-19b*) and *miR-20a*. While *miR-20a* exhibited minimal oncogenic collaboration with *c-myc*, *miR-19b* and *c-myc* resulted in highly malignant B lymphomas with nearly complete penetrance (median survival 87 d; *P* < 0.0001, log rank test) (Fig. 1D). Given the sequence homology between *miR-19a* and *miR-19b* and their 1-nt divergence at a region nonessential for miRNA target recognition, it is possible that *miR-19a* can also accelerate *c-myc*-induced lymphomagenesis. Similar to *mir-19a/20a/19b*, *miR-19b* phenocopied the oncogenic effects of *mir-17-19b*. Interestingly, mice overexpressing *miR-19b* exhibited a slightly longer life span after reconstitution (Fig. 3C, below) when compared with those overexpressing *miR-17-19b*, a difference likely due to functional cooperation among *miR-19b*, *miR-19a*, and possibly *miR-18a*.

Histopathological and immunophenotyping analyses confirmed the phenotypic similarities among the *Eμ-myc/miR-19b* (*Eμ-myc/19b*), *Eμ-myc/mir-19a/20a/19b* (*Eμ-myc/19a/20a/19b*), and *Eμ-myc/mir-17-19b* (*Eμ-myc/17-19b*) lymphomas. These mice developed advanced lymphomas, with massive enlargement of lymph nodes, splenic hyperplasia, and leukemia. In all cases, lymphoma cells invaded the thymus and bone marrow, as well as visceral organs outside the lymphoid compartment, including the liver, lung, and, occasionally, kidney (Fig. 2A; He et al. 2005). While control *Eμ-myc* lymphomas exhibited a high mitotic index accompanied by extensive cell death as shown by TUNEL staining (Fig. 2B; Supplemental Fig. S3), the *Eμ-myc/19a/20a/19b* and *Eμ-myc/19b* lymphomas, similar to *Eμ-myc/17-19b* lymphomas, had greatly reduced apoptosis without affecting cell proliferation (Fig. 2B; Supplemental Fig. S3). Although *mir-17-92* has been implicated to promote cell proliferation in other cellular contexts (Ventura et al. 2008), *mir-17-19b*, *mir-19a/20a/19b*, and *miR-19b* overexpression did not enhance cell proliferation in the *Eμ-myc* model. The lack of proliferative effects in the B-lymphoma cells is likely due to the high level of basal proliferation resulting from *c-myc* overexpression. Additionally, control *Eμ-myc* mice frequently develop more

Olive et al.
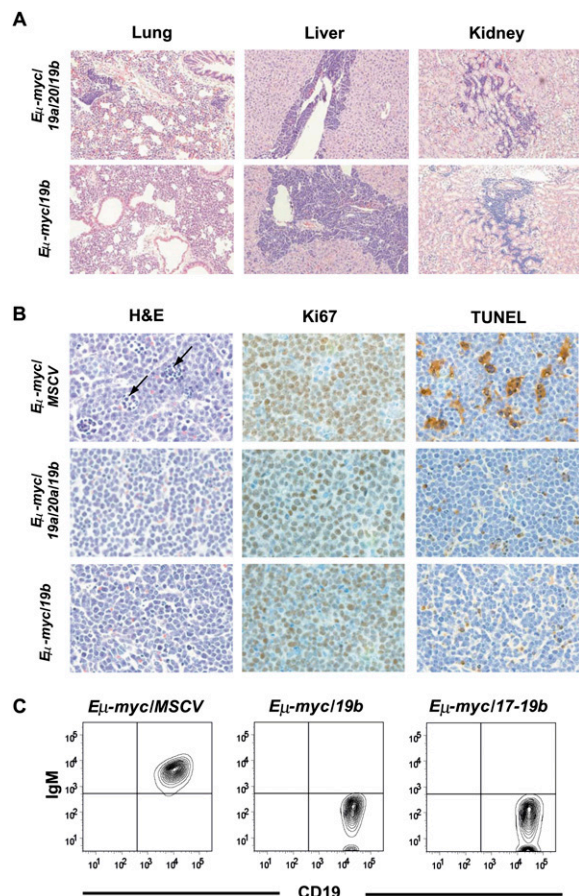
Figure 2. *Eμ-myc/17-19* and *Eμ-myc/19b* lymphomas have similar pathological and immunological features. (*A*) *Eμ-myc/19b* lymphomas are highly invasive. H&E staining of the liver, lung, and kidney showed aggressive invasion by *Eμ-myc/19b* tumor cells, which was highly analogous to that of the *Eμ-myc/19a/20a/19b* lymphomas. In particular, both perivascular and parenchymal invasion of the liver were observed. (*B*) Overexpression of *miR-19b* represses *c-myc*-induced apoptosis. The *Eμ-myc/19b* and *Eμ-myc/19a/20a/19b* lymphomas had similar proliferation rates to those of *Eμ-myc/MSCV* controls, demonstrated by Ki67 staining. However, exogenous expression of *miR-19b* or *mir-19a/20/19b* greatly decreased apoptosis in the *Eμ-myc* tumors, confirmed by TUNEL and H&E staining of *Eμ-myc/17-19* lymph node tumors. The "starry sky" morphology of cell clusters undergoing apoptosis (black arrows), a hallmark of *Eμ-myc/MSCV* lymphomas, was absent in *Eμ-myc/19b* and *Eμ-myc/19a/20a/19b* tumors. (*C*) *miR-19b* and *mir-17-19b* preferably transform progenitor B cells. Flow cytometric immunophenotyping of representative *Eμ-myc*, *Eμ-myc/17-19*, and *Eμ-myc/19* lymphomas. While the majority of *Eμ-myc* tumors consisted of CD19-positive and IgM-positive B cells, the *Eμ-myc/19b* and *Eμ-myc/17-19* tumor cells bore cellular characteristics of progenitor B cells, positive for CD19 but not for surface IgM.

mature B-cell lymphomas, but the *Eμ-myc/19b*, *Eμ-myc/19a/20a/19b*, and *Eμ-myc/17-19b* tumors were derived primarily from progenitor B cells (Fig. 2C; Supplemental Table S1; Supplemental Fig. S2), suggesting a functional preference for these miRNAs to transform B-cell progenitors under our experimental conditions. These observations were consistent with the B-cell phenotypes in the

mir-17-92 knockout mice, in which the pro-B-to-pre-B transition was marked by extensive apoptosis (Ventura et al. 2008).

miR-19 *components are required for the oncogenic activity of* mir-17-92

Among all of the *mir-17-92* components, *miR-19* is sufficient for accelerating *c-myc*-induced lymphomagenesis. To determine whether *miR-19* miRNAs are also necessary for the oncogenic effects of *mir-17-19b*, we introduced mutations into *miR-19a* and *miR-19b* within the *mir-17-19b* construct (designated as *mir-17-19b-Mut19*). In so doing, we disrupted the hairpin stem of both *miR-19a* and *miR-19b* to abolish the biogenesis of *miR-19* miRNAs while preventing generation of cryptic miRNAs. These mutations specifically disabled *miR-19* biogenesis, without affecting that of *miR-17*, *miR-18a*, and *miR-20a* within the same construct (Fig. 3A,B). Consistent with *miR-19* being the key oncogenic component, the *miR-19* mutations greatly compromised the oncogenic capacity of *mir-17-19b*, causing delayed tumor onset, incomplete penetrance, and extended life span (median survival 141 d; $P < 0.001$, log rank test) (Fig. 3C). In *Eμ-myc/mir-17-19b-Mut19* (*Eμ-myc/17-19b-Mut19*) animals that ultimately developed late-onset lymphomas, the *miR-19* mutations significantly compromised cell survival without affecting cell proliferation (Fig. 3D,E; Supplemental Fig. S3). In comparison, tumors derived from oncogenic collaboration between *c-myc* and *mir-17-19b* or *miR-19b* alone exhibited greatly reduced apoptosis (Figs. 2B, 3D,E). The *miR-19* mutations not only disrupted cell survival, but also compromised the ability of *mir-17-19b* to preferentially transform progenitor B cells. This was suggested by the immunophenotyping analyses on *Eμ-myc/17-19b-Mut19* B-cell tumors, which exhibited more cell type heterogeneity compared with *Eμ-myc/17-19b* tumors (Supplemental Table S1). Taken together, these findings establish *miR-19* miRNAs as the key oncogenic component within *mir-17-92*, promoting tumorigenesis seemingly through the repression of *c-myc*-induced apoptosis.

miR-19 *specifically dampens the expression level of the tumor suppressor* Pten

miR-19 is the key oncogenic component of *mir-17-92*, and therefore *miR-19*-specific targets are likely to mediate the oncogenic effects of *mir-17-92*. Among hundreds of *miR-19* targets predicted by TargetScan and RNA22 (Lewis et al. 2005; Miranda et al. 2006; Grimson et al. 2007), the tumor suppressor *Pten* is a prominent candidate, due to its important functions in promoting apoptosis and tumor suppression. *Pten* is a negative regulator of the PI3K signaling. In response to a variety of extracellular signals, the PI3K pathway elicits diverse cellular responses to promote cell survival, rapid proliferation, and cell growth. *Pten* has been implicated as a target of *mir-17-92* by luciferase reporter assays and Western analyses in cell culture-based experiments (Takakura
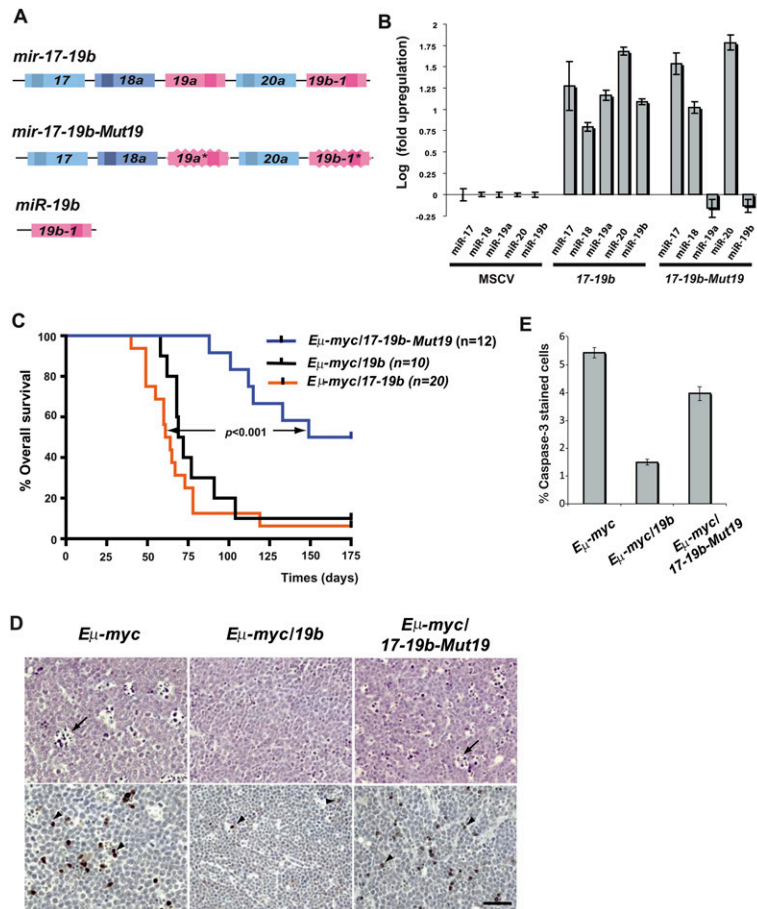
Figure 3. *miR-19* miRNAs are essential for the oncogenic activity of *mir-17-19b*. (*A*) A schematic representation of the gene structural organization of *mir-17-19b*, *mir-17-19b-Mut19*, and *miR-19b*. 19a* and 19b* indicate *miR-19* mutations. (*B*) *miR-19* mutations specifically affected *miR-19* expression in *mir-17-19b*. 3T3 cells were infected with MSCV-*mir-17-19b*, MSCV-*mir-17-19b-Mut19*, or control MSCV vectors. Expression levels of *miR-17*, *miR-18a*, *miR-19a*, *miR-20a*, and *miR-19b* were determined using TaqMan miRNA assays. *miR-19* mutations specifically affected the expression of *miR-19a* and *miR-19b*, but not that of the adjacent *mir-17-19b* components. Error bars indicate SD ($n = 3$). (*C*) *miR-19* is both necessary and sufficient for the oncogenic effect of *mir-17-19b*. Overexpression of *miR-19b* and *mir-17-19b* accelerated *c-myc*-induced lymphomagenesis to a similar degree, shown in Kaplan-Meier curves as the percentage of overall survival. Mutations in *miR-19* greatly decreased the oncogenic activity of *mir-17-19b* in the *Eμ-myc* model. We compared the oncogenic effects of *mir-17-19b*, *miR-19b*, and *mir-17-19b-Mut19* in the same adoptive transfer experiment. (*D*) *miR-19* is both necessary and sufficient for the cell survival effect of *mir-17-19b* in vivo. Representative lymphomas from *Eμ-myc*, *Eμ-myc/19b*, and *Eμ-myc/17-19b-Mut19* were stained for H&E and caspase-3, which indicated that the *miR-19* mutations significantly compromised cell survival effects of *mir-17-19b*, while *miR-19b* overexrepssion suppresses apoptosis. The *Eμ-myc/19b* and *Eμ-myc/17-19b-Mut19* tumors shown here were both IgM-negative B lymphomas. (Arrow) "Starry sky" feature of apoptotic tumor cells; (arrowhead) apoptotic cells with positive caspase-3 staining. Bar, 50 μm. (*E*) Quantification of caspase-3 staining of representative tumors from *D* as percentage of positive cells. For *Eμ-myc/19b* and *Eμ-myc/17-19b-Mut19* tumors, only IgM-negative tumors were selected for this comparison ($n = 3$; error bars represent SEM).

et al. 2008; Xiao et al. 2008). However, it is not clear how individual *mir-17-92* components contribute to the repression of *Pten* and, more importantly, whether the down-regulation of *Pten* by *mir-17-92* leads to any functional impact on cell survival.

Overexpression of *miR-19b* and *mir-17-19b*—but not *miR-17*, *miR-18a*, *miR-20a*, or MSCV control—significantly down-regulated the endogenous level of *Pten* mRNA and protein in NIH-3T3 cells (Fig. 4C,D). Similarly, *Pten* down-regulation by *miR-19b* and *mir-17-19b* was observed in mouse primary B-cell culture (Supplemental Fig. S4B). The ability of *mir-17-19b* to down-regulate *Pten* in both cell types depended on the intact *miR-19* components within this cluster, since *mir-17-19b/Mut19* failed to dampen *Pten* expression in either 3T3 cells or primary B-cell culture (Fig. 4E,F; Supplemental Fig. S4A,B). These findings suggest that *miR-19* is the *mir-17-92* component that is both necessary and sufficient to mediate *Pten* repression. Interestingly, the level of *Pten* repression by *miR-19* was also dependent on cell types and physiological contexts, possibly due to differences in basal levels of *miR-19* and *Pten* expression (Hwang et al. 2009; data not shown).

The human *PTEN* 3′ untranslated region (UTR) contains two *miR-19*-binding sites (Fig. 4A; Miranda et al. 2006). A luciferase reporter, when fused with the wild-type human *PTEN* 3′UTR, was significantly repressed by overexpression of *miR-19b*, but not by *miR-17*, *miR-18a*, *miR-20a*, or *miR-1* control (Fig. 4B). Mutations of one or both *miR-19*-binding sites in the luc-*PTEN* 3′UTR construct either partially or completely derepressed the luciferase reporter when coexpressed with *miR-19b* (Fig. 4A,B). These findings suggest that direct binding between *miR-19* and *PTEN* 3′UTR is required for PTEN repression by *miR-19*.

miR-19 *functionally antagonizes* Pten *to promote cell survival*

miR-19 is evolutionarily conserved across many vertebrate species (Griffiths-Jones 2006). Between *Xenopus* and mammals, the sequences of *miR-19a* and *miR-19b* are identical, and two putative *miR-19*-binding sites are also present in the *Xenopus pten* mRNA. These observations implicate a selective pressure to preserve the *pten* regulation by *miR-19* during ~350 million years of

Olive et al.
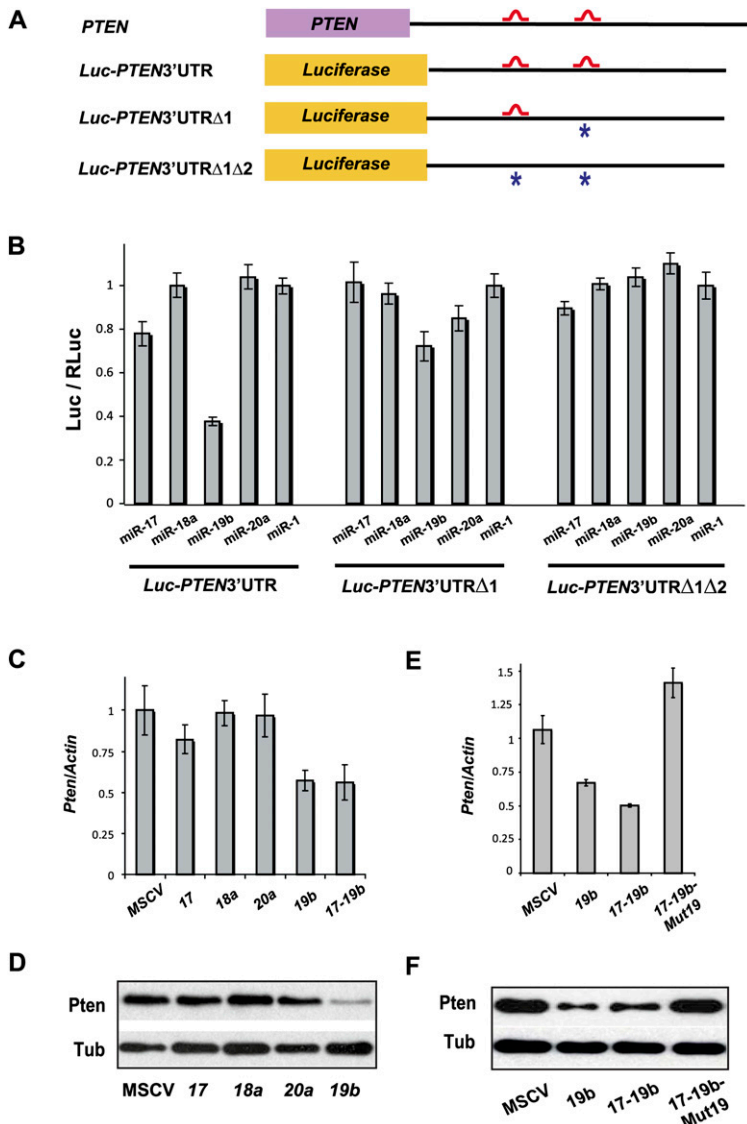
Figure 4. *Pten* is a *mir-17-19b* target specifically regulated by *miR-19*. (*A*) Schematic representation of the *PTEN* 3′UTR and its *miR-19*-binding sites. Two *miR-19*-binding sites (shown in red) can be found in the human *PTEN* 3′UTR. The *PTEN* 3′UTR with mutations (designated with asterisks) at one (*PTEN3′ UTR*Δ1) or both (*PTEN3′UTR*Δ1Δ2) *miR-19* sites, as well as the wild-type counterpart (*PTEN3′UTR*), were each cloned downstream from a luciferase reporter (*Luc*). (*B*) Specific repression of *Luc-PTEN3′UTR* reporter by *miR-19*. *Luc-PTEN3′UTR* was cotransfected with mimics of *miR-17*, *miR-18a*, *miR-19b*, *miR-20a*, and control *miR-1*. Only *miR-19b* significantly repressed the reporter expression. Cotransfection with a luciferase construct carrying one mutated *miR-19b* site in the *PTEN* 3′UTR (*Luc-PTEN3′UTR*Δ1) partially derepressed the Luc reporter, and cotransfection of a construct with mutations in both *miR-19* sites (*Luc-PTEN3′UTR*Δ1Δ2) completely derepressed the Luc reporter. (*C,D*) *miR-19b* specifically represses endogenous *Pten* expression level. Using real-time PCR analysis (*C*) and Western analysis (*D*), down-regulation of endogenous *Pten* mRNA and protein can be detected in serum-starved NIH-3T3 cells infected with *miR-19b* and *mir-17-19b*. In comparison, overexpression of *miR-17*, *miR-18a*, *miR-20a*, and control vector (MSCV) in these cells has minimal effects on the endogenous *Pten* level. (*E,F*) *miR-19* is both necessary and sufficient to mediate the *Pten* repression by *mir-17-19b*. Repression of endogenous *Pten* mRNA (*E*) and protein (*F*) can be detected in serum-starved NIH-3T3 cells infected with *miR-19b* and *mir-17-19b*. In comparison, *mir-17-19b-Mut19* failed to repress the endogenous *Pten* level.

evolution. To determine whether *Pten* down-regulation by *miR-19* had any functional impact, we examined their functional interaction using an in vivo apoptosis assay in *Xenopus* embryos.

Not only is *miR-19* conserved at the sequence level in *Xenopus*, its anti-apoptotic function is also preserved, evident by its ability to repress hydroxyurea-induced cell death. When subjected to hydroxyurea treatment, *Xenopus* embryos undergo apoptosis, often characterized by a whitish color, cell blebbing, and disruption of cell adhesion after the mid-blastula transition (Walker and Harland 2009). Injection of *miR-19b* considerably rescued hydroxyurea-induced apoptosis (Fig. 5A,B). Consistent with *Pten* being a key target of *miR-19*, injection of *miR-19* and *pten* individually gave rise to opposite phenotypes, with *miR-19* promoting cell survival (Fig. 5A,B) and *pten* inducing apoptosis (Fig. 5C,D). Coinjection of *miR-19b* and *pten*, however, significantly rescued *pten*-induced apoptosis, but a mutated *miR-19b* (*mut-19b*)

with an altered seed sequence failed to impact the *pten* function (Fig. 5C,D). When we introduced mutations in the two *miR-19*-binding sites in the *pten* cDNA without affecting *pten* protein coding, the mutated *pten* mRNA (*pten-mut*) retained the ability to potently induce cell death. In this case, *miR-19* injection failed to rescue the apoptotic effects of *pten-Mut* (Fig. 5E,F). Altogether, our findings indicate that the repression of *Pten* by *miR-19* occurs not only at the expression level, but also at the functional level, both of which are dependent on the intact *miR-19*-binding sites within the *Pten* mRNA.

miR-19 *activates the Akt–mTOR pathway both in vitro and in vivo*

PTEN is a tumor suppressor that is mutated or deleted in multiple tumor types with high frequency (Di Cristofano and Pandolfi 2000; Knobbe et al. 2008). It acts to repress the intracellular level of phosphatidylinositol-3,4,5-trisphosphate
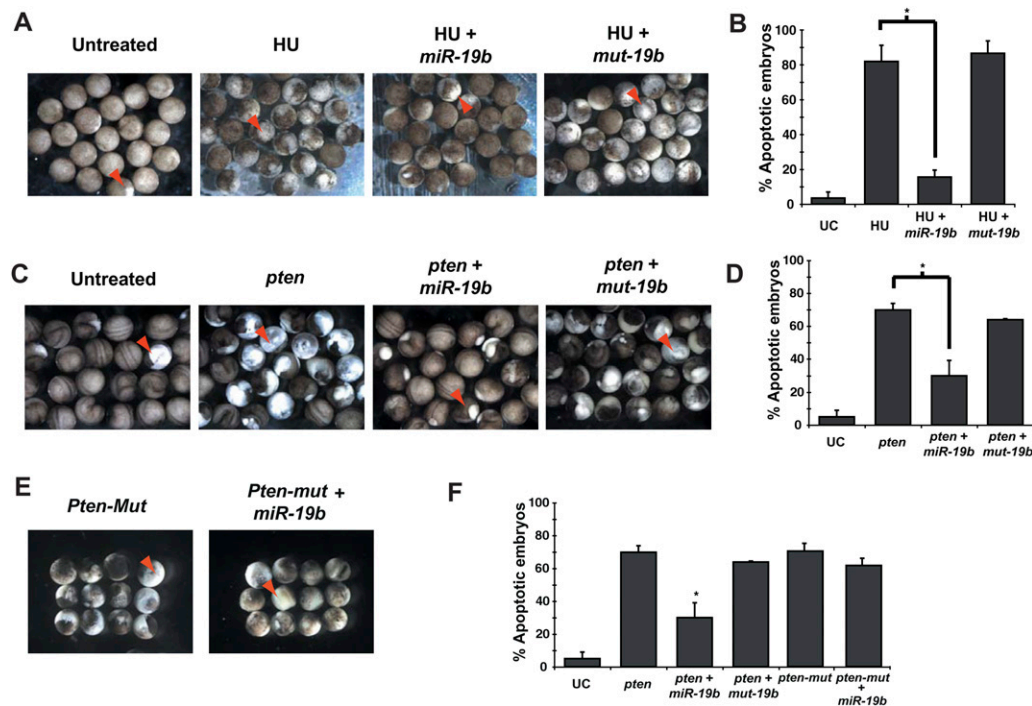
Figure 5. *miR-19b* functionally antagonizes *pten*-induced apoptosis in *Xenopus* embryos. (*A,B*) *miR-19b* rescues hydroxyurea (HU)-induced apoptosis in *X. laevis* embryos. Injection of *miR-19b* mimics into *X. laevis* embryos rescued apoptosis caused by hydroxyurea treatment. The mutated *miR-19b* with an altered seed region (*mut-19b*) failed to rescue hydroxyurea-induced apoptosis. Embryos undergoing apoptosis were marked by cell blebbing, disruption of cell adhesion, and a characteristic white color (red arrowhead). Hydroxyurea-treated embryos appeared more pigmented than control embryos, largely due to developmental arrest. (*B*) Apoptosis was quantified for untreated and hydroxyurea-treated embryos, as well as the hydroxyurea-treated embryos coinjected with either *miR-19b* mimics or *mut-19b* mimics ($n = 3$ experiments with >25 embryos in each group; [*] $P < 0.05$). (*C,D*) Injection of *miR-19b* rescued *pten*-induced apoptosis in *Xenopus* embryos. Injection of full-length *pten* mRNA into *Xenopus* embryos led to widespread apoptosis. Injection of *miR-19b*, but not *mut-19b*, significantly rescued the proapoptotic effect of *pten*. (*E,F*) Disruption of base-pairing between *miR-19* and *pten* mRNA abolished their functional antagonism. Mutations in the *miR-19*-binding sites within the *pten* mRNA (*pten-mut*) did not abrogate the proapoptotic effects of *pten*, but did eliminate the ability of *miR-19b* to repress the apoptosis ($n = 3$ experiments with >25 embryos in each group; [*] $P < 0.05$). All error bars represent SEM.

in cells, thus negatively regulating the PI3K pathway and its downstream effectors, Akt and mTOR (Comer and Parent 2002; Rossi and Weissman 2006). Consistent with the ability of *miR-19* to repress *Pten* expression and function, *miR-19b* overexpression in NIH-3T3 cells specifically activated the PI3K pathway, leading to increased phosphorylation of Akt without affecting the overall level of Akt (Fig. 6A). *miR-19b* or *mir-17-19b* overexpression also caused a significant increase in phosphorylation of S6 ribosomal protein due to the activated mTOR pathway (Supplemental Fig. S4D). Surprisingly, *miR-17* and *miR-20a* overexpression slightly increased the phospho-S6 level compared with the vector control, but this increase might be achieved through a mechanism independent of Pten or Akt (Fig. 6A,B). Using Western analyses and immunohistochemistry assays, a high level of phospho-S6 protein was observed in a cohort of *Eµ-myc/19b* and *Eµ-myc/17-19b* tumors, suggesting that *miR-19* and *mir-17-19b* were able to activate the mTOR pathway in vivo (Fig. 6C,D), at least in part through the repression on *Pten*. In comparison, the control *Eµ-myc* tumors generally exhibited a low level of phospho-S6

protein, although a certain degree of heterogeneity existed among different tumors. Although *mir-17-19b* and *miR-19b* were equally potent in inducing phospho-S6 in vitro (Supplemental Fig. S4D), the effect of *mir-17-19b* in vivo was more potent (Fig. 6C,D), possibly due to a degree of cooperative effects from the other miRNA components. The late-onset *Eµ-myc/17-19b-Mut19* lymphomas had varying levels of phospho-S6, yet this cohort of lymphomas as a whole exhibited a decrease in the phospho-S6 level compared with *Eµ-myc/17-19b* tumors (Supplemental Fig. S4E).

Although *Pten* deficiency in mice frequently gives rise to T-cell malignancy, *Pten* heterozygosity appears to partially phenocopy *mir-17-19b* overexpression, and cooperates with *c-myc* in the *Eµ-myc* model to moderately accelerate B lymphomagenesis (Wendel et al. 2006). However, the oncogenic effect of *miR-19b* or *mir-17-19b* is more potent than *Pten* heterozygosity in the *Eµ-myc* lymphoma model. *Pten* is a haploinsufficient tumor suppressor whose dosage proportionally impacts its tumor suppressor activity and inversely correlates with tumor progression in a cell type-dependent manner

Olive et al.
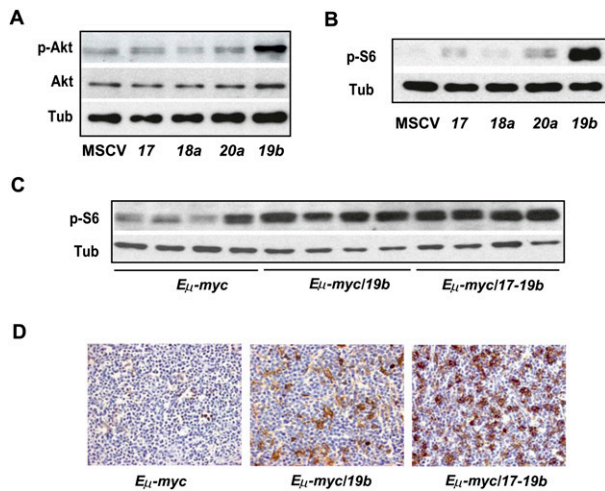
Figure 6. *miR-19* and *mir-17-19b* activates the Akt–mTOR pathway. (*A*) *miR-19* is a key *mir-17-19b* component to activate the Akt–mTOR pathway. Using Western analysis, increased phospho-Akt level was detected in serum-starved 3T3 cells infected with *miR-19b*, but not *miR-17*, *miR-18a*, *miR-20a*, and the control vector (MSCV). In comparison, the overall Akt level was not affected by *miR-19b*. (*B*) *miR-19* induces an increase in phosphorylation of S6 ribosomal protein. Enforced expression of *miR-19b* strongly promoted the S6 phosphorylation as compared with the rest of *mir-17-19b* components. (*C*,*D*) Enforced *miR-19b* or *mir-17-19b* expression in the *Eµ-myc* model led to an increased level of phospho-S6 in lymphomas. Cells derived from the *Eµ-myc*, *Eµ-myc/19b*, and *Eµ-myc/17-19b* lymphomas were analyzed by Western (*C*) and immunohistochemistry (*D*). Both *Eµ-myc/19b* and *Eµ-myc/17-19b* lymphomas exhibited a high level of phospho-S6, although *mir-17-19b* seemed to have a stronger effect. In comparison, *Eµ-myc* tumors exhibited a low level of phospho-S6 and more variation among different samples, possibly reflecting the differences in the secondary oncogenic lesions. In all Western analyses, tubulin (Tub) was used as a normalization control.

(Trotman et al. 2003). It is likely that *miR-19b* or *mir-17-19b* overexpression, when compared with *Pten* heterozygosity, causes greater *Pten* repression (Supplemental Fig. S4C), and thus a stronger B-cell transformation in the *Eµ-myc* model. Interestingly, in non-Hodgkin's B-cell lymphomas (NHLs) including Burkitt's lymphoma and DLBCL, recurring deletions and rearrangements of 10q23, which harbors *PTEN*, are observed in 5%–10% of patients (Butler et al. 1999). In addition, the reduction or loss of *PTEN* expression is often associated with inferior survival (Abubaker et al. 2007; Robledo et al. 2009). These findings implicate the importance of the *PTEN* pathway in the progression and prognosis of specific human B-cell malignancies. Besides *PTEN* deletion and mutations, *mir-17-92*-mediated *PTEN* repression may be an additional mechanism to disrupt the *PTEN* function and to promote malignant transformation in human B cells. In line with this hypothesis, a recent study described a subset of DLBCLs in which the amplification of *mir-17-92* and the deletion of *PTEN* are mutually exclusive (Lenz et al. 2008).

Discussion

The small size of miRNAs, combined with their imperfect base-pairing for target recognition, allows miRNAs to regulate many mRNA targets. The strong cooperation between *miR-19* and *c-myc* can result from the collective impacts on many *miR-19* targets, of which *Pten* is a key target, but it may not be the only one. Given the robust induction of phospho-S6 by *miR-19*, it is possible that other negative regulators of the PI3K–AKT–mTOR pathway, in addition to *Pten*, are coordinately regulated. It is also conceivable that additional pathways regulated by *miR-19* could synergize with down-regulated *Pten* to promote cell survival and malignant transformation. Increasing evidence suggests that the dosage of tumor suppressor genes has a significant impact on their functional readout. A number of tumor suppressors are haploinsufficient, and hypomorphic mutations in tumor suppressors are frequent in cancer (Payne and Kemp 2005). Given the importance of miRNAs in human cancer and their unique mechanism of action, partial repression of tumor suppressors is likely a novel mechanism through which miRNA oncogenes promote malignant transformation.

Polycistronic gene structure is frequently observed in miRNA loci (Ambros 2004; He and Hannon 2004; Zamore and Haley 2005). Since each miRNA has the potential to regulate hundreds of target mRNAs, a miRNA polycistron containing multiple components may possess a greater capacity for gene regulation, thus yielding pleiotropic biological effects through complex mechanisms of coordination. In the context of B-cell transformation in the *Eµ-m*yc model, *miR-19* miRNAs are identified as the key oncogenic components of *mir-17-92* to cooperate with *c-myc*. The other *mir-17-92* components either are dispensable for oncogenesis, or, as in the case of *miR-18a*, may play an accessory role to enhance oncogenic potential. As a strong oncogene, *mir-17-92* can regulate multiple cellular processes to favor malignant transformation, causing decreased cell death, rapid cell proliferation, and increased angiogenesis (He et al. 2005; O'Donnell et al. 2005; Dews et al. 2006; Ventura et al. 2008). However, it remains unclear how this polycistronic miRNA regulates coordinated biological processes to achieve malignant transformation. It is conceivable that individual *mir-17-92* components function cooperatively to impact multiple cellular processes, although more complex mechanisms of coordination may also exist. A recent study indicates that *miR-17* overexpression in mice decreases cell proliferation, adhesion, and migration, raising a possibility that components of *mir-17-92* can both positively and negatively regulate the same cellular process to achieve homeostasis (Shan et al. 2009). It is possible that cell types and biological contexts may also determine the exact mechanisms of coordination among polycistronic miRNA components. We are just beginning to understand the functional complexity of polycistronic miRNAs, which have an enormous capacity for gene regulation and complex coordination among different components. The unique gene structure of these miRNA polycistrons

can ultimately underlie the molecular basis for their pleiotropic functions in the oncogenic and tumor suppressor network.

Materials and methods

Molecular construction of mir-17-92 subclusters

The subclusters of *mir-17-92* were amplified by PCR and subsequently cloned into the XhoI and EcoRI sites of the MSCV retrovirus vectors. In these vectors, miRNAs were placed downstream from the LTR promoter, which is followed by either a SV40-GFP cassette (for all in vivo experiments) or a PGK-Puro-Ires-GFP cassette (for all in vitro experiments) (Hemann et al. 2005). To construct the MSCV-*17-19b/Mut19* vector, a 12-nt mutation was introduced into the hairpin stem of *pre-mir-19a* and *pre-mir-19b* using the QuickChangeXL mutagenesis kit (Strategene). For the MSCV-*17-19b/Mut19* vector, the loss of *miR-19* expression and the normal expression of the other *mir-17-19b* components were validated using the TaqMan miRNA assays (Applied Biosystems).

Adoptive transfer of Eμ-myc HSPCs for lymphomagenesis

Fetal liver-derived HSPCs were isolated from embryonic day 13.5–15.5 (E13.5–E15.5) *Eμ-myc*/+ embryos, and were transduced with MSCV alone or MSCV expressing various *mir-17-92* subclusters. The MSCV retroviral vector used in our studies contains a SV40-GFP cassette that allows us to monitor transduced HSPCs both in vitro and in vivo. Infected HSPCs were subsequently transplanted into 8- to 9-wk-old, lethally irradiated C57BL/6 recipient mice. Tumor onset was subsequently monitored by weekly palpation, and tumor samples were either collected into formalin for histopathological studies, or prepared as single-cell suspension for FACS analysis.

Luciferase assays

Human *PTEN* 3′UTR were amplified from the genomic DNA (forward primer, 5′-CACCAAGATGGCACTTTCC CGTTT-3′; reverse primer, 5′-TGGCAAACATGTTCAA GAGGAGCT-3′), which contains two *miR-19*-binding sites that are also conserved in mice. Mutagenesis of these two *miR-19*-binding sites was carried out using the QuickChangeXL mutagenesis kit (Strategene). The wild-type *PTEN* 3′UTR, as well as the mutated *PTEN* 3′UTR fragments, were each cloned downstream from a firefly luciferase reporter. These firefly luciferase constructs that contain either the wild-type or the mutated *PTEN* 3′UTR were each transfected into the Dicer-deficient Hct116 cells (Cummins et al. 2006), together with a Renilla luciferase construct for normalization control, and 50 nM miRNA mimics for *mir-17*, *mir-18*, *miR-19b*, *miR-20a*, and *mir-1*, respectively. These miRNA mimics were generated by annealing two complementary RNA oligos (IDT). Luciferase activity of each construct was determined by dual luciferase assay (Promega) 48 h post-transfection.

Cell culture

NIH-3T3 cells were cultured in DMEM with 10% bovine serum, and were kept 30%–40% confluent throughout the entire cell culture experiment. Primary B cells were prepared from mouse bone marrows, and were cultured in RPMI medium with 10% fetal bovine serum (FBS), 50 μM β-mercaptoethanol, and 2 ng/mL Il-7. NIH-3T3 cells and mouse primary B-cell cultures were infected by MSCV retroviruses expressing *mir-17-92* subclusters, and were selected by puromycin for 2 d. Serum-starved NIH-3T3 cells were prepared by incubating the cells with DMEM without serum for 12 h before harvesting the cell lysate. MSCV-infected primary B cells were sorted based on GFP, and were then subjected to Western analyses or real-time PCR analyses as described below.

Real-time PCR analysis and Western analysis

TaqMan miRNA assays (Applied Biosystems) were used to measure the level of mature miRNAs. The mRNA level for *Pten* (forward primer, 5′-CACAATTCCCAGTC AGAGGCGC-3′; reverse primer, 5′-GCTGGCAGACCA CAAACTGAGGA-3′) was determined using real-time PCR analysis with SYBR (Applied Biosystems). Actin was used as a normalization control in all our RT-QPCR experiments (forward primer, 5′-GATCTGGCACCACA CCTTCT-3′; reverse primer, 5′-GGGGTGTTGAAGGT CTCAAA-3′). For Western analyses, Pten (Cell Signaling), Akt (Cell Signaling), phospho-Akt (Ser473; Cell Signaling), and phospho-S6 (Cell Signaling) antibodies were used at 1:1000, and tubulin antibody (Sigma) was used at 1:4000.

Histopathology

Tissue samples were fixed in formalin, embedded in paraffin, sectioned into 5-μm sections, and stained with haematoxylin and eosin (H&E). For Ki-67 (rabbit anti-Ki67; NovoCastra), caspase-3 (AF835; R&D Systems), and PCNA (MS-106P; Lab Vision Corp.) detection, representative sections were deparaffinized and rehydrated in graded alcohols before being subjected to antigen retrieval treatment in a vegetable steamer. Detection of antibody staining was carried out following standard procedures from the avidin-biotin immunoperoxidase methods. Diaminobenzidine (Invitrogen) was used as the chromogen and haematoxylin was used as the nuclear counterstain. Analysis of the apoptotic rate by TUNEL assay was performed according to a published protocol (Di Cristofano et al. 1998).

Flow cytometry

Lymphoma cells harvested from the animals were resuspended in 10% FBS/phosphate-buffered saline (PBS) to reach a concentration of 10^7 cells per milliliter. Twenty microliters of the cell suspension were stained with various antibodies diluted in 10% FBS/PBS for 1 h. Subsequently, cells were washed with 2% FBS/PBS and resuspended in 10% FBS/PBS for flow cytometry analysis. Antibodies

used for our FACS analyses include PE anti-mouse IgM (eBioscience, 12-5790), APC-Cy7 B220 (BD Pharmingen, 552094), CD4 APC-Cy7 (BD Pharmingen, 552051), PE-CD8 (BD Pharmingen, 553032), PE-CD25 (BD Pharmingen, 553866), and APC-CD19 (Biolegend, 115511).

Apoptotic assays

Xenopus laevis eggs were collected and fertilized, and embryos were cultured by standard procedures. The *miR-19b* mimics were produced from the annealing products of 5′-UGUGCAAAUCCAUGCAAAACUGA-3′ and 5′-AGUUUUGCAGGUUUGCAUCCAUU-3′ (IDT). Two complimentary RNA oligos were combined and diluted to a stock concentration of 1 µg/µL, heated for 1 min to 80°C, and then allowed to cool to room temperature to form duplexes. The same was done to generate the mutated *miR-19* mimics, *mut-19b*, using 5′-UCAGGU AAUCCAUGCAAAACUGA-3′ and 5′-AGUUUUGCAG GUUACCUUCGAUU-3′. The *Pten-mut* construct was made by two consecutive QuickChange reactions of accession plasmid BC161129 with primers 5′-ACAAATT TAGCTGCAGAGTAG-3′ and 5′-GGTCTTCAAACGG ATACTGAG-3′, and 5′-GCAGAGTGAGGGGAGCGG GT-3′ and 5′-CGGGGAAAGGTTGGCACCCG-3′. *Xenopus tropicalis pten* and *pten-mut* RNAs were made using the mMessage SP6 kit (Ambion) on Not1-cut plasmid. Embryos were injected into both cells at the two-cell stage with 2 ng of each RNA. Hydroxyurea (Sigma) was diluted to a final concentration of 15 mM and embryos were treated from 2 h post-fertilization until stage 10.5. All embryos undergoing apoptosis of any cells were scored as positive.

Acknowledgments

References

Abubaker J, Bavi PP, Al-Harbi S, Siraj AK, Al-Dayel F, Uddin S, Al-Kuraya K. 2007. PIK3CA mutations are mutually exclusive with PTEN loss in diffuse large B-cell lymphoma. *Leukemia* **21:** 2368–2370.

Adams JM, Harris AW, Pinkert CA, Corcoran LM, Alexander WS, Cory S, Palmiter RD, Brinster RL. 1985. The c-myc oncogene driven by immunoglobulin enhancers induces lymphoid malignancy in transgenic mice. *Nature* **318:** 533–538.

Ambros V. 2004. The functions of animal microRNAs. *Nature* **431:** 350–355.

Baek D, Villen J, Shin C, Camargo FD, Gygi SP, Bartel DP. 2008. The impact of microRNAs on protein output. *Nature* **455:** 64–71.

Bartel DP. 2009. MicroRNAs: Target recognition and regulatory functions. *Cell* **136:** 215–233.

Butler MP, Wang SI, Chaganti RS, Parsons R, Dalla-Favera R. 1999. Analysis of PTEN mutations and deletions in B-cell non-Hodgkin's lymphomas. *Genes Chromosomes Cancer* **24:** 322–327.

Calin GA, Sevignani C, Dumitru CD, Hyslop T, Noch E, Yendamuri S, Shimizu M, Rattan S, Bullrich F, Negrini M, et al. 2004. Human microRNA genes are frequently located at fragile sites and genomic regions involved in cancers. *Proc Natl Acad Sci* **101:** 2999–3004.

Chi SW, Zang JB, Mele A, Darnell RB. 2009. Argonaute HITS-CLIP decodes microRNA–mRNA interaction maps. *Nature* **460:** 479–486.

Comer FI, Parent CA. 2002. PI 3-kinases and PTEN: How opposites chemoattract. *Cell* **109:** 541–544.

Cummins JM, He Y, Leary RJ, Pagliarini R, Diaz LA Jr, Sjoblom T, Barad O, Bentwich Z, Szafranska AE, Labourier E, et al. 2006. The colorectal microRNAome. *Proc Natl Acad Sci* **103:** 3687–3692.

Dews M, Homayouni A, Yu D, Murphy D, Sevignani C, Wentzel E, Furth EE, Lee WM, Enders GH, Mendell JT, et al. 2006. Augmentation of tumor angiogenesis by a Myc-activated microRNA cluster. *Nat Genet* **38:** 1060–1065.

Di Cristofano A, Pandolfi PP. 2000. The multiple roles of PTEN in tumor suppression. *Cell* **100:** 387–390.

Di Cristofano A, Pesce B, Cordon-Cardo C, Pandolfi PP. 1998. Pten is essential for embryonic development and tumour suppression. *Nat Genet* **19:** 348–355.

Farh KK, Grimson A, Jan C, Lewis BP, Johnston WK, Lim LP, Burge CB, Bartel DP. 2005. The widespread impact of mammalian microRNAs on mRNA repression and evolution. *Science* **310:** 1817–1821.

Filipowicz W, Bhattacharyya SN, Sonenberg N. 2008. Mechanisms of post-transcriptional regulation by microRNAs: Are the answers in sight? *Nat Rev Genet* **9:** 102–114.

Griffiths-Jones S. 2006. miRBase: The microRNA sequence database. *Methods Mol Biol* **342:** 129–138.

Grimson A, Farh KK, Johnston WK, Garrett-Engele P, Lim LP, Bartel DP. 2007. MicroRNA targeting specificity in mammals: Determinants beyond seed pairing. *Mol Cell* **27:** 91–105.

Hayashita Y, Osada H, Tatematsu Y, Yamada H, Yanagisawa K, Tomida S, Yatabe Y, Kawahara K, Sekido Y, Takahashi T. 2005. A polycistronic microRNA cluster, miR-17-92, is overexpressed in human lung cancers and enhances cell proliferation. *Cancer Res* **65:** 9628–9632.

He L, Hannon GJ. 2004. MicroRNAs: Small RNAs with a big role in gene regulation. *Nat Rev Genet* **5:** 522–531.

He L, Thomson JM, Hemann MT, Hernando-Monge E, Mu D, Goodson S, Powers S, Cordon-Cardo C, Lowe SW, Hannon GJ, et al. 2005. A microRNA polycistron as a potential human oncogene. *Nature* **435:** 828–833.

He L, He X, Lim LP, de Stanchina E, Xuan Z, Liang Y, Xue W, Zender L, Magnus J, Ridzon D, et al. 2007a. A microRNA component of the p53 tumour suppressor network. *Nature* **447:** 1130–1134.

He L, He X, Lowe SW, Hannon GJ. 2007b. microRNAs join the p53 network—Another piece in the tumour-suppression puzzle. *Nat Rev Cancer* **7:** 819–822.

Hemann MT, Bric A, Teruya-Feldstein J, Herbst A, Nilsson JA, Cordon-Cardo C, Cleveland JL, Tansey WP, Lowe SW. 2005. Evasion of the p53 tumour surveillance network by tumour-derived MYC mutants. *Nature* **436:** 807–811.

Hwang HW, Wentzel EA, Mendell JT. 2009. Cell–cell contact globally activates microRNA biogenesis. *Proc Natl Acad Sci* **106:** 7016–7021.

Inomata M, Tagawa H, Guo YM, Kameoka Y, Takahashi N, Sawada K. 2009. MicroRNA-17-92 down-regulates expression of distinct targets in different B-cell lymphoma subtypes. *Blood* **113:** 396–402.

Johnson SM, Grosshans H, Shingara J, Byrom M, Jarvis R, Cheng A, Labourier E, Reinert KL, Brown D, Slack FJ. 2005. RAS is regulated by the let-7 microRNA family. *Cell* **120:** 635–647.

Kim VN, Han J, Siomi MC. 2009. Biogenesis of small RNAs in animals. *Nat Rev Mol Cell Biol* **10:** 126–139.

Knobbe CB, Lapin V, Suzuki A, Mak TW. 2008. The roles of PTEN in development, physiology and tumorigenesis in mouse models: A tissue-by-tissue survey. *Oncogene* **27:** 5398–5415.

Kota J, Chivukula RR, O'Donnell KA, Wentzel EA, Montgomery CL, Hwang HW, Chang TC, Vivekanandan P, Torbenson M, Clark KR, et al. 2009. Therapeutic microRNA delivery suppresses tumorigenesis in a murine liver cancer model. *Cell* **137:** 1005–1017.

Kumar MS, Erkeland SJ, Pester RE, Chen CY, Ebert MS, Sharp PA, Jacks T. 2008. Suppression of non-small cell lung tumor development by the let-7 microRNA family. *Proc Natl Acad Sci* **105:** 3903–3908.

Lenz G, Wright GW, Emre NC, Kohlhammer H, Dave SS, Davis RE, Carty S, Lam LT, Shaffer AL, Xiao W, et al. 2008. Molecular subtypes of diffuse large B-cell lymphoma arise by distinct genetic pathways. *Proc Natl Acad Sci* **105:** 13520–13525.

Lewis BP, Shih IH, Jones-Rhoades MW, Bartel DP, Burge CB. 2003. Prediction of mammalian microRNA targets. *Cell* **115:** 787–798.

Lewis BP, Burge CB, Bartel DP. 2005. Conserved seed pairing, often flanked by adenosines, indicates that thousands of human genes are microRNA targets. *Cell* **120:** 15–20.

Lu J, Getz G, Miska EA, Alvarez-Saavedra E, Lamb J, Peck D, Sweet-Cordero A, Ebert BL, Mak RH, Ferrando AA, et al. 2005. MicroRNA expression profiles classify human cancers. *Nature* **435:** 834–838.

Miranda KC, Huynh T, Tay Y, Ang YS, Tam WL, Thomson AM, Lim B, Rigoutsos I. 2006. A pattern-based method for the identification of microRNA binding sites and their corresponding heteroduplexes. *Cell* **126:** 1203–1217.

Navarro A, Bea S, Fernandez V, Prieto M, Salaverria I, Jares P, Hartmann E, Mozos A, Lopez-Guillermo A, Villamor N, et al. 2009. MicroRNA expression, chromosomal alterations, and immunoglobulin variable heavy chain hypermutations in Mantle cell lymphomas. *Cancer Res* **69:** 7071–7078.

O'Donnell KA, Wentzel EA, Zeller KI, Dang CV, Mendell JT. 2005. c-Myc-regulated microRNAs modulate E2F1 expression. *Nature* **435:** 839–843.

Ota A, Tagawa H, Karnan S, Tsuzuki S, Karpas A, Kira S, Yoshida Y, Seto M. 2004. Identification and characterization of a novel gene, C13orf25, as a target for 13q31-q32 amplification in malignant lymphoma. *Cancer Res* **64:** 3087–3095.

Robledo C, Garcia JL, Caballero D, Conde E, Arranz R, Flores T, Grande C, Rodriguez J, Garcia E, Saez AI, et al. 2009. Array comparative genomic hybridization identifies genetic regions associated with outcome in aggressive diffuse large B-cell lymphomas. *Cancer* **115:** 3728–3737.

Rossi DJ, Weissman IL. 2006. Pten, tumorigenesis, and stem cell self-renewal. *Cell* **125:** 229–231.

Schmitt CA, Wallace-Brodeur RR, Rosenthal CT, McCurrach ME, Lowe SW. 2000. DNA damage responses and chemo-

sensitivity in the E mu-myc mouse lymphoma model. *Cold Spring Harb Symp Quant Biol* **65:** 499–510.

Selbach M, Schwanhausser B, Thierfelder N, Fang Z, Khanin R, Rajewsky N. 2008. Widespread changes in protein synthesis induced by microRNAs. *Nature* **455:** 58–63.

Shan SW, Lee DY, Deng Z, Shatseva T, Jeyapalan Z, Du WW, Zhang Y, Xuan JW, Yee SP, Siragam V, et al. 2009. MicroRNA MiR-17 retards tissue growth and represses fibronectin expression. *Nat Cell Biol* **11:** 1031–1038.

Tagawa H, Seto M. 2005. A microRNA cluster as a target of genomic amplification in malignant lymphoma. *Leukemia* **19:** 2013–2016.

Tagawa H, Karube K, Tsuzuki S, Ohshima K, Seto M. 2007. Synergistic action of the microRNA-17 polycistron and Myc in aggressive cancer development. *Cancer Sci* **98:** 1482–1490.

Takakura S, Mitsutake N, Nakashima M, Namba H, Saenko VA, Rogounovitch TI, Nakazawa Y, Hayashi T, Ohtsuru A, Yamashita S. 2008. Oncogenic role of miR-17-92 cluster in anaplastic thyroid cancer cells. *Cancer Sci* **99:** 1147–1154.

Trotman LC, Niki M, Dotan ZA, Koutcher JA, Di Cristofano A, Xiao A, Khoo AS, Roy-Burman P, Greenberg NM, Van Dyke T, et al. 2003. Pten dose dictates cancer progression in the prostate. *PLoS Biol* **1:** E59. doi: 10.1371/journal.pbio.0000059.

Ventura A, Young AG, Winslow MM, Lintault L, Meissner A, Erkeland SJ, Newman J, Bronson RT, Crowley D, Stone JR, et al. 2008. Targeted deletion reveals essential and overlapping functions of the miR-17 through 92 family of miRNA clusters. *Cell* **132:** 875–886.

Walker JC, Harland RM. 2009. microRNA-24a is required to repress apoptosis in the developing neural retina. *Genes & Dev* **23:** 1046–1051.

Wendel HG, Malina A, Zhao Z, Zender L, Kogan SC, Cordon-Cardo C, Pelletier J, Lowe SW. 2006. Determinants of sensitivity and resistance to rapamycin–chemotherapy drug combinations in vivo. *Cancer Res* **66:** 7639–7646.

Xiao C, Srinivasan L, Calado DP, Patterson HC, Zhang B, Wang J, Henderson JM, Kutok JL, Rajewsky K. 2008. Lymphoproliferative disease and autoimmunity in mice with increased miR-17-92 expression in lymphocytes. *Nat Immunol* **9:** 405–414.

Zamore PD, Haley B. 2005. Ribo-gnome: The big world of small RNAs. *Science* **309:** 1519–1524.

miR-19 is a key oncogenic component of *mir-17-92*

Virginie Olive, Margaux J. Bennett, James C. Walker, et al.

Supplemental Material	http://genesdev.cshlp.org/content/suppl/2009/11/30/23.24.2839.DC1
Related Content	**Tumorigenicity of the miR-17-92 cluster distilled** Gijs van Haaften and Reuven Agami Genes Dev. January , 2010 24: 1-4 **Genetic dissection of the miR-17<92 cluster of microRNAs in Myc-induced B-cell lymphomas** Ping Mu, Yoon-Chi Han, Doron Betel, et al. Genes Dev. December , 2009 23: 2806-2811
References	This article cites 52 articles, 14 of which can be accessed free at: http://genesdev.cshlp.org/content/23/24/2839.full.html#ref-list-1 Articles cited in: http://genesdev.cshlp.org/content/23/24/2839.full.html#related-urls
License	
Email Alerting Service	Receive free email alerts when new articles cite this article - sign up in the box at the top right corner of the article or **click here.**